

GNSS-R Soil Moisture Retrieval Method Based on Transformer Fusion Network

Song Dai, Dongmei Song, Bin Wang

College of Oceanography and Space Informatics, China University of Petroleum (East China), Qingdao, China

Email: b22160011@s.upc.edu.cn, songdongmei@upc.edu.cn, wangbin007@upc.edu.cn

How to cite this paper: Dai, S., Song, D.M. and Wang, B. (2025) GNSS-R Soil Moisture Retrieval Method Based on Transformer Fusion Network. *Journal of Computer and Communications*, 13, 201-216.
<https://doi.org/10.4236/jcc.2025.136014>

Received: May 18, 2025

Accepted: June 27, 2025

Published: June 30, 2025

Abstract

Global Navigation Satellite System-Reflectometry (GNSS-R) remote sensing technology, with its advantages of low cost, short revisit cycle, and high-precision positioning, has been widely applied in soil moisture retrieval. To improve the accuracy of soil moisture retrieval, this paper proposes a Transformer-based fusion network (Transformer Fusion Network, TF-NET). TF-NET leverages a multi-head self-attention mechanism to extract deep features from GNSS-R observation data and auxiliary data, and enhances the feature correlation between different data sources through a cross-attention mechanism, thereby achieving high-precision soil moisture prediction. In this study, the Yellow River Delta was selected as the experimental area, and the Cyclone Global Navigation Satellite System (CYGNSS) and Tianmu Satellite were chosen as the primary data sources. Due to the complementary spatial coverage of the two satellites, soil moisture was retrieved separately from each satellite data, and the results were spatially combined. In the validation process, soil moisture observation data from the Soil Moisture Active Passive (SMAP) satellite were used as reference data. Experimental results indicate that the joint use of CYGNSS and Tianmu satellite data significantly improves the accuracy and reliability of soil moisture retrieval.

Keywords

GNSS-R, CYGNSS, Tianmu, SMAP, Soil Moisture Retrieval

1. Introduction

Traditional soil moisture monitoring methods, including gravimetric, resistivity, and neutron methods, were among the earliest applied techniques. However, these methods are labor-intensive, costly, and limited to local areas. With the continuous development of remote sensing technology, remote sensing has played an in-

creasingly important role in soil moisture retrieval due to its wide observation range, high spatiotemporal resolution, and easy data sharing [1]-[4]. Among remote sensing methods, optical remote sensing, with its shorter wavelength, has weaker signal penetration and is easily affected by weather. In contrast, microwave remote sensing, with its longer wavelength, can penetrate clouds and rain, enabling all-weather observation, and is therefore widely used.

Microwave remote sensing includes both passive and active microwave remote sensing. Passive microwave remote sensing primarily involves radiometers, such as the Soil Moisture Active Passive (SMAP) Satellite launched by NASA and the Soil Moisture and Ocean Salinity (SMOS) Satellite launched by the European Space Agency. Both SMAP and SMOS satellites have a spatial resolution of 36 km and a temporal resolution of 3 days for object detection. Active microwave remote sensing, represented by satellites like the Sentinel-1 launched by ESA, offers a spatial resolution of 1 km and a temporal resolution of 6 - 12 days [5]. However, neither passive nor active microwave remote sensing can simultaneously provide high spatiotemporal resolution, and their development costs are relatively high.

Compared with microwave remote sensing technology, the Global Navigation Satellite System Reflectometry (GNSS-R) is a satellite remote sensing technique characterized by high spatiotemporal resolution, strong signal penetration, and low cost. It obtains information on reflective surfaces by processing and analyzing signals reflected from the ocean, land, or other objects [6]. GNSS-R technology is commonly used for monitoring the ocean and retrieving terrestrial physical parameters, such as biomass estimation [7], sea ice monitoring [8], ocean altimetry [9], and soil moisture retrieval [10]-[13]. Due to the strong surface penetration capability of L-band signals, GNSS-R technology is particularly suitable for detecting soil moisture changes.

With the continuous advancement of GNSS-R technology, spaceborne GNSS-R techniques have been increasingly applied to soil moisture retrieval. Currently, numerous studies focus on retrieving surface soil moisture using CYGNSS data (Chew and Small [14], 2018; Kim and Lakshmi [15], 2018; Clarizia *et al.* [16], 2019). These methods typically establish empirical relationships between CYGNSS-derived reflectivity or signal-to-noise ratio (SNR) and soil moisture data obtained from SMAP or in-situ networks. However, due to the influence of various complex factors, the relationship between GNSS-R signals and soil moisture is inherently more complex and nonlinear. Compared to linear models, machine learning algorithms are more suitable for revealing these intrinsic nonlinear relationships. Therefore, many researchers employ machine learning techniques to conduct soil moisture retrieval studies. Due to their strong nonlinear mapping capability, machine learning methods have been widely used in GNSS-R soil moisture retrieval and have achieved good retrieval accuracy.

In recent years, with the rapid development of deep learning, its adaptive learning ability and capability to deeply explore the intrinsic patterns in data have been widely demonstrated. Scholars have successfully achieved GNSS-R soil moisture

retrieval using deep learning methods. As deep learning techniques evolve, the Transformer model has gradually expanded from natural language processing to computer vision. When processing two-dimensional images, the Transformer model [17] can effectively utilize positional information through the self-attention mechanism, establishing connections between different regions. In GNSS-R technology, the Delay-Doppler Map (DDM) is a critical observation result that forms a two-dimensional image with time delay and Doppler shift as coordinates. Since information at different delays and Doppler shifts may be correlated or contrasted, applying the Transformer model to process DDM images helps extract comprehensive information on soil moisture variation.

To achieve high-precision soil moisture retrieval, this paper proposes a Transformer-based fusion network (Transformer Fusion Network, TF-NET) using spaceborne GNSS-R data. In the TF-NET framework, the self-attention mechanism extracts intrinsic features from DDM data and auxiliary data, while the cross-attention mechanism enhances feature correlations between different modals, effectively capturing the global context and long-range dependencies of spaceborne GNSS-R multi-modal data.

To maximize the fusion advantages of TF-NET, this study further proposes a joint dataset based on CYGNSS and Tianmu satellite data. In the Yellow River Delta region, these two satellite data sources differ significantly in spatial distribution and orbital coverage but complement each other effectively, overcoming the limitations of single satellite data in spatial coverage and spatiotemporal resolution. By constructing this joint dataset, the model can more comprehensively capture soil moisture variation in the study area, thereby effectively improving the accuracy of soil moisture retrieval.

The remainder of this paper is organized as follows. Section 2 introduces the study area and the datasets used. Section 3 provides a detailed description of the proposed method. Section 4 presents the experimental results and analysis. Finally, Section 5 concludes the study.

2. Data Preparation

2.1. Study Area

This study selects the Yellow River Delta Efficient Ecological Economic Zone (referred to as the Yellow River Delta) as the experimental area. The geographical coordinates range from 36°25'N to 38°14'N and 116°55'E to 120°19'E, as shown in **Figure 1**. The Yellow River Delta is located at the intersection of the historical Yellow River alluvial plain and the northern coastal area of Shandong Province. The region is characterized by flat terrain and diverse geomorphological types, including rivers, wetlands, saline-alkali land, farmland, and coastal tidal flats. These diverse ecological landscapes result in a complex ecological environment with significant ecological functions.

Additionally, the Yellow River Delta is a core area of the Bohai Economic Rim and has experienced rapid economic development in recent years. Frequent hu-

man activities have led to an increasing demand for regional water resources, further exacerbating the vulnerability of the ecosystem. The climate in this area belongs to the warm temperate continental monsoon climate, characterized by uneven annual precipitation. The significant difference in precipitation between the rainy and dry seasons directly results in a highly complex and dynamic spatiotemporal distribution of soil moisture.

Furthermore, the widespread distribution of saline-alkali land in the region poses a greater challenge for accurate soil moisture monitoring. Therefore, there is an urgent need for a high-precision, stable, and reliable soil moisture retrieval technology to accurately grasp the dynamic changes in soil moisture in this region. Such a technology would provide essential data support and scientific decision-making guidance for ecological environment protection, saline-alkali land management, agricultural production optimization, and rational allocation of water resources in the Yellow River Delta.

2.2. Data Introduction

To fully exploit the scientific potential of GNSS-R technology in the field of soil moisture retrieval, the National Aeronautics and Space Administration (NASA) successfully launched the CYGNSS satellite constellation in December 2016. The constellation consists of eight small satellites, each equipped with a signal receiver featuring four branch channels, allowing simultaneous signal observation across 32 channels. The average revisit period of the CYGNSS constellation is approximately 7 hours, and its spatial resolution varies with surface roughness. When the reflective surface is relatively smooth, the spatial resolution can reach $3.5 \text{ km} \times 0.5 \text{ km}$; however, when the surface roughness is significant, such as on extremely rough ocean surfaces, the spatial resolution decreases to about $25 \text{ km} \times 25 \text{ km}$.

In contrast, the Tianmu satellite constellation is China's first low-orbit meteorological observation constellation constructed under a commercial model, operated by Aerospace Tianmu (Chongqing) Satellite Technology Co., Ltd., a subsidiary of the China Aerospace Science and Industry Corporation. The first batch of satellites was successfully launched in 2022. The Tianmu-1 satellite constellation is equipped with GNSS occultation and GNSS ocean reflectometry (GNSS-R) payloads, capable of receiving signals from the BeiDou, GPS, Galileo, and GLONASS navigation systems. This enables global, all-weather, high spatiotemporal resolution remote sensing observations of the atmosphere, oceans, and surface environments. The spatial resolution of the Tianmu-1 satellite constellation is approximately $200 \text{ km} \times 200 \text{ km}$, with a temporal resolution of 6 hours.

Additionally, the validation data and auxiliary data used in this study were obtained from the Soil Moisture Active Passive (SMAP) satellite, launched by NASA in January 2015. The core mission of the SMAP satellite is to detect soil moisture within the 0 - 5 cm surface depth. Although the active radar on the SMAP satellite experienced a hardware failure on July 7, 2015, the onboard microwave radiome-

ter has continued to function steadily, providing high-precision soil moisture data. Given that the SMAP satellite, like CYGNSS and Tianmu satellites, utilizes L-band signals for observation, and since SMAP data has demonstrated superior accuracy and reliability among existing soil moisture observation products, this study uses SMAP soil moisture observations as the reference data for verifying retrieval results.

The SMAP satellite collects observation data through microwave radiometers with spatial resolutions of 9 km and 36 km, and releases soil moisture products based on the EASE-Grid 2.0 system. This study uses the Enhanced Level 3 SMAP data product with a spatial resolution of 9 km \times 9 km. Besides soil moisture information, the dataset also includes auxiliary variables such as vegetation optical thickness, vegetation water content, surface roughness, and surface temperature. This study specifically utilizes five key variables from the SMAP dataset: soil moisture, vegetation optical thickness, vegetation water content, surface roughness, and surface temperature. Among these, soil moisture data serves as the reference to evaluate the accuracy of retrieval results, while the other four variables are used as auxiliary features to enhance the accuracy of soil moisture retrieval.

Due to the limited temporal and spatial availability of Tianmu satellite observation data, this study selected CYGNSS, Tianmu, and SMAP data from May, June, July, and September 2023 to ensure temporal synchronization and maintain the scientific validity and consistency of the retrieval analysis.

2.3. Data Preprocessing

To extract features closely related to soil moisture as model inputs, comprehensive data preprocessing was performed on CYGNSS, Tianmu satellite, and SMAP data. During the preprocessing process, strict quality control procedures were followed to clean and filter the raw observational data, removing outliers and low-quality data to ensure high reliability and consistency of the input data.

To further improve the accuracy of soil moisture retrieval, rigorous data preprocessing was applied to both Tianmu satellite and CYGNSS observational data. The primary goal of preprocessing was to eliminate data with poor quality or potential errors, thereby preventing low-quality data from interfering with model training and prediction, which could adversely affect accuracy and stability.

1) Firstly, when processing CYGNSS data, observations with an incidence angle greater than 65° were excluded. At such high incidence angles, the reliability of reflected signals significantly decreases, making it highly prone to large errors. These data points lack representativeness in feature extraction and model training. Therefore, to ensure model performance, observations with high incidence angles were strictly removed.

2) Second, data with a receiver antenna gain below 0 dB were removed, since low gain weakens signal reception and leads to inaccurate results. To maintain data quality, only observations meeting the gain criteria were kept.

3) Additionally, observations with a Signal-to-Noise Ratio (SNR) below 0 were

discarded, as negative SNR values indicate noise dominance, lacking valid signal information. Including such data could negatively impact model accuracy.

By following these preprocessing steps, noise and low-quality data were effectively filtered out, ensuring reliable and consistent input data for soil moisture retrieval. **Table 1** summarizes all the data used in this study.

Table 1. Feature reference table.

Data source	Feature representation	Feature name
CYGNSS/Tianmu	DDM	Delay doppler map
	SR	Surface reflectance
	Time	Observation time
	Angle	Incident angle
	DDMA	Mean DDM
	Peak	Peak DDM
	SNR	Signal to Noise Ratio
	Lon	longitude
	Lat	Latitude
	Les	Leading edge slope
SMAP	VOD	Vegetation optical thickness
	VWC	Surface water content
	Rough	Surface roughness
	Tem	Surface temperature

3. Proposed Method

To capture the global contextual information and long-range dependencies embedded in GNSS-R data, and thereby further enhance the accuracy of soil moisture retrieval, this study proposes a multi-modal fusion method based on spaceborne GNSS-R data, named the Transformer Fusion Network (TF-NET).

TF-NET is specifically designed to integrate the complementary features of one-dimensional auxiliary data and two-dimensional DDM data, making full use of their unique characteristics to improve prediction performance. The network takes one-dimensional auxiliary data and two-dimensional DDM data as inputs and outputs the predicted soil moisture, as illustrated in **Figure 1**.

TF-NET first utilizes a Convolutional Neural Network (CNN) to efficiently extract spatial local information from DDM data and deep features from auxiliary data, achieving structural alignment and unified embedding of different modal features. Subsequently, the Transformer Fusion module extracts single-modal features while enhancing the complementarity of multi-modal data, enabling the modeling of long-range dependencies and information fusion. The framework of TF-NET will be described in detail in the following sections.

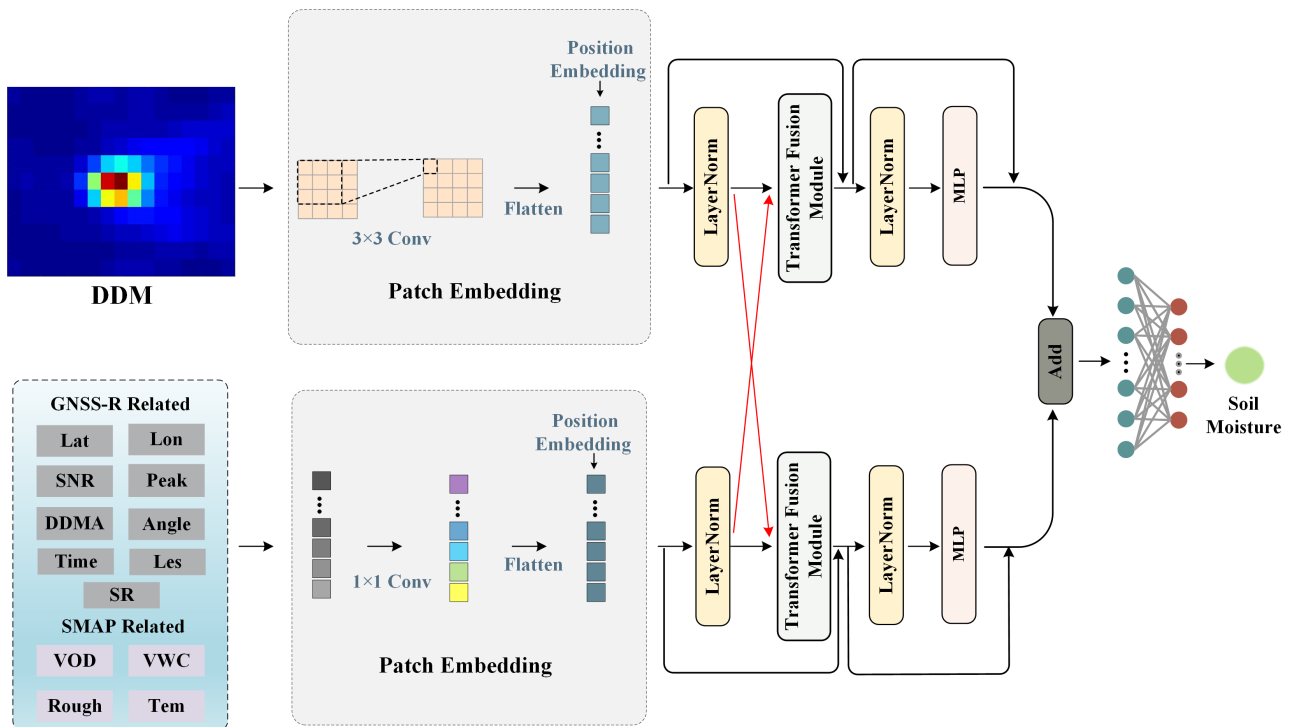


Figure 1. TF-NET framework diagram.

3.1. Transformer Fusion Module

TF-NET employs a dual-branch multi-feature input module to separately process one-dimensional auxiliary data and two-dimensional DDM data, effectively extracting semantic features and spatial structure information from each data type. This ensures a unified dimensional embedding representation, providing a solid foundation for subsequent data fusion.

The Transformer Fusion module is the core component of the TF-NET model, specifically designed to fuse one-dimensional auxiliary data and two-dimensional DDM data to fully extract multi-modal data features and their interrelationships. This module primarily consists of two critical mechanisms: multi-head self-attention and multi-head cross-attention, which play a key role in feature extraction and multi-modal data fusion.

The multi-head self-attention mechanism is mainly used to extract single-modal features by processing the one-dimensional auxiliary data and two-dimensional DDM data separately. For the one-dimensional auxiliary data, this mechanism effectively captures the feature representation by modeling the feature correlations within the auxiliary data space, thereby fully leveraging the deep information embedded in the one-dimensional features. When processing the two-dimensional DDM data, the multi-head self-attention mechanism extracts spatial local features and long-range dependencies by focusing on the relationships between different spatial positions, thus achieving comprehensive feature extraction from DDM images. This mechanism ensures feature alignment within each single modality, laying a solid foundation for subsequent multi-modal fusion.

On the other hand, the multi-head cross-attention mechanism is designed to enhance the feature interaction between one-dimensional auxiliary data and two-dimensional DDM data. Since these two types of data differ significantly in their feature space and expression forms, the cross-attention mechanism employs a mutual attention strategy that allows one-dimensional and two-dimensional features to learn from and complement each other, forming close associations at the feature level. This mechanism significantly improves the complementarity between multi-modal data, which is essential for accurately capturing the variation characteristics of multi-source information in soil moisture retrieval.

Within the Transformer Fusion module, the hybrid multi-head attention mechanism simultaneously handles self-attention and cross-attention, enabling dynamic feature fusion. This mechanism not only facilitates information exchange within the same data patch but also enhances the complementary relationships between one-dimensional and two-dimensional features. The introduction of this dual attention structure equips the model with greater robustness against feature heterogeneity and noise, significantly improving the accuracy and stability of soil moisture predictions.

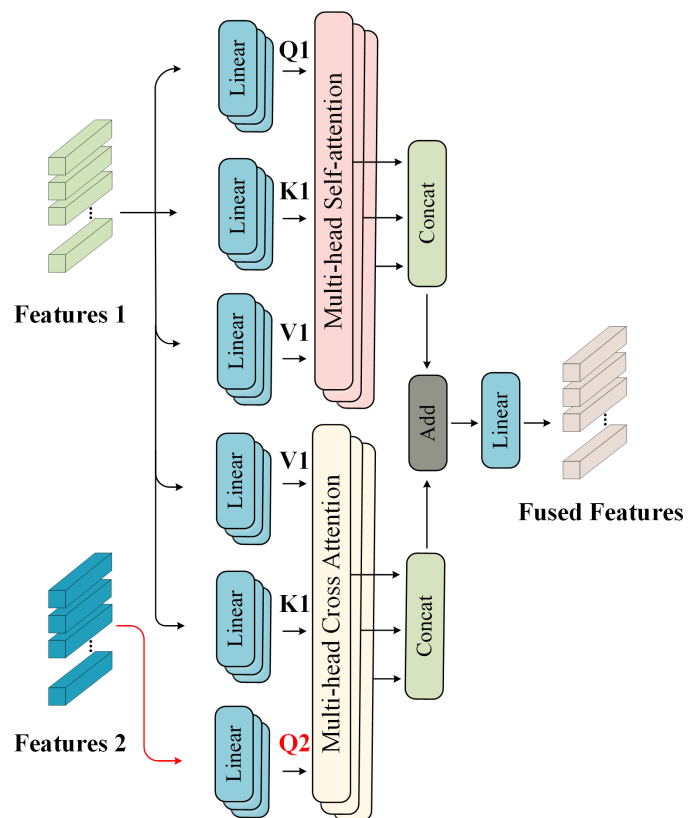


Figure 2. Schematic diagram of the Transformer fusion module.

As shown in **Figure 2**, the architecture of the Transformer Fusion module clearly demonstrates the modular integration of the self-attention and cross-attention mechanisms within the network structure. **Figure 3** further details the Trans-

former attention calculation process, emphasizing the interaction and feature fusion between one-dimensional auxiliary data and two-dimensional DDM data. These visual representations intuitively illustrate how the TF-NET model utilizes the hybrid attention mechanism to achieve outstanding performance in soil moisture retrieval tasks.

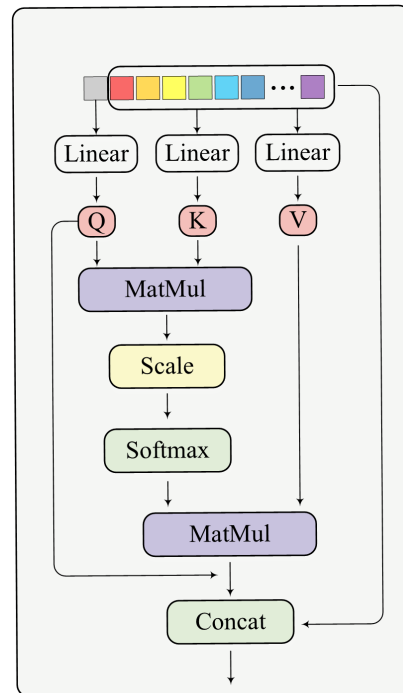


Figure 3. Schematic diagram of Transformer attention calculation.

3.2. Hyperparameter Setting

The experimental setup was conducted on a computer equipped with a GeForce GTX 4080 16G GPU and an Intel i9-13900H CPU. The experiments were implemented using the PyTorch framework on the PyCharm platform. The Adam optimizer was employed to update network gradients, with the initial learning rate set to 0.001. The number of iterations was set to 100. As the number of training iterations increased, the loss value gradually decreased and eventually stabilized.

To eliminate the impact of random factors in the experiments, each experiment was repeated ten times, and the average value was calculated.

To evaluate the retrieval performance of the network model, the Root Mean Square Error (RMSE) and Correlation Coefficient (R) were introduced as evaluation metrics. The calculation formulas are shown in Equations (1) and (2).

$$RMSE = \sqrt{\frac{1}{n} \sum_{i=1}^n (f_i - y_i)^2} \quad (1)$$

$$R = \frac{\sum_{i=1}^n (f_i - \bar{f})(y_i - \bar{y})}{\sqrt{\sum_{i=1}^n (f_i - \bar{f})^2 (y_i - \bar{y})^2}} \quad (2)$$

where f_i represents the actual observation value, y_i represents the model prediction value, n denotes the total number of sample points, and \bar{f} and \bar{y} are the mean values of the predicted and actual observation values, respectively.

4. Experimental Results and Analysis

4.1. Experimental Result

In this study, the SMAP data was used to comprehensively validate the effectiveness of the TF-NET model for soil moisture retrieval in the Yellow River Delta region.

Firstly, **Figure 4** presents scatter plots of soil moisture predictions made by the TF-NET model based on CYGNSS and Tianmu satellite data, respectively. The predicted values from the model are visually compared with the SMAP observation reference data to evaluate the accuracy of the model predictions.

During the experiments, the training and testing data were randomly divided in a ratio of 8:2 to ensure that the model possesses good generalization capability.

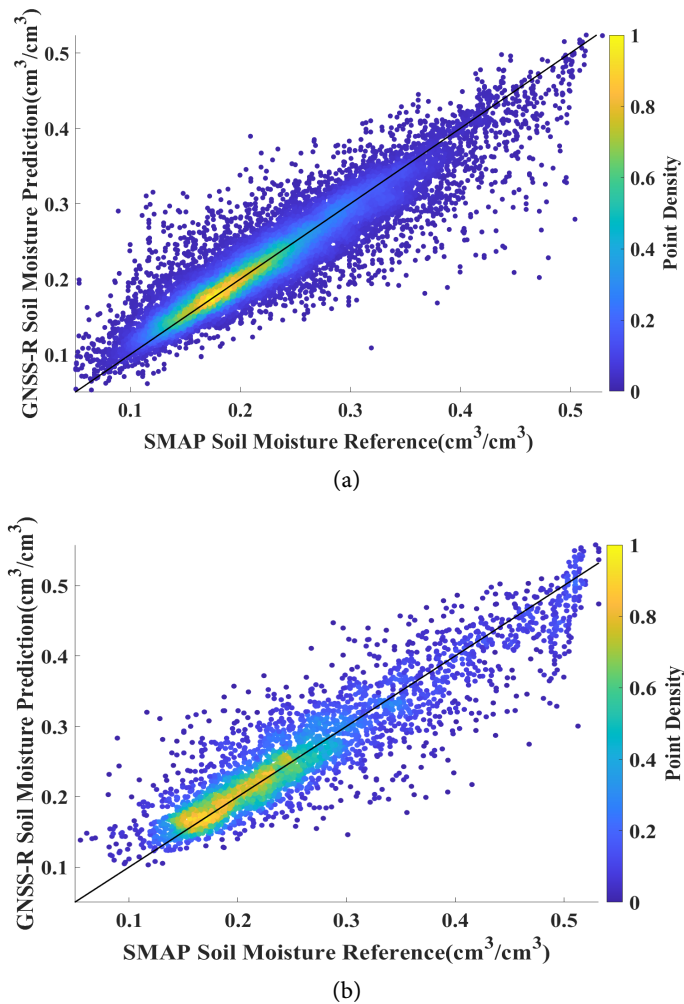


Figure 4. Scatter images between the model prediction results and the reference data (a) CYGNSS, (b) Tianmu.

To further evaluate the predictive performance of the TF-NET model for specific months, this study designed a time series experiment. The data from May, June, and July were used to train the model, while the September data, which was not involved in the training process, was selected as an independent test set. This setup aimed to investigate the model's ability to predict the spatial distribution of soil moisture in an unseen month.

Figure 5 visually presents the spatial coverage of CYGNSS and Tianmu satellite data in September 2023. It can be clearly observed that the CYGNSS satellite exhibits severe data gaps in the northern part of the Yellow River Delta, while the Tianmu satellite shows insufficient data acquisition in the southern part of the region. The complementary nature of the spatial coverage between the two satellites is evident.

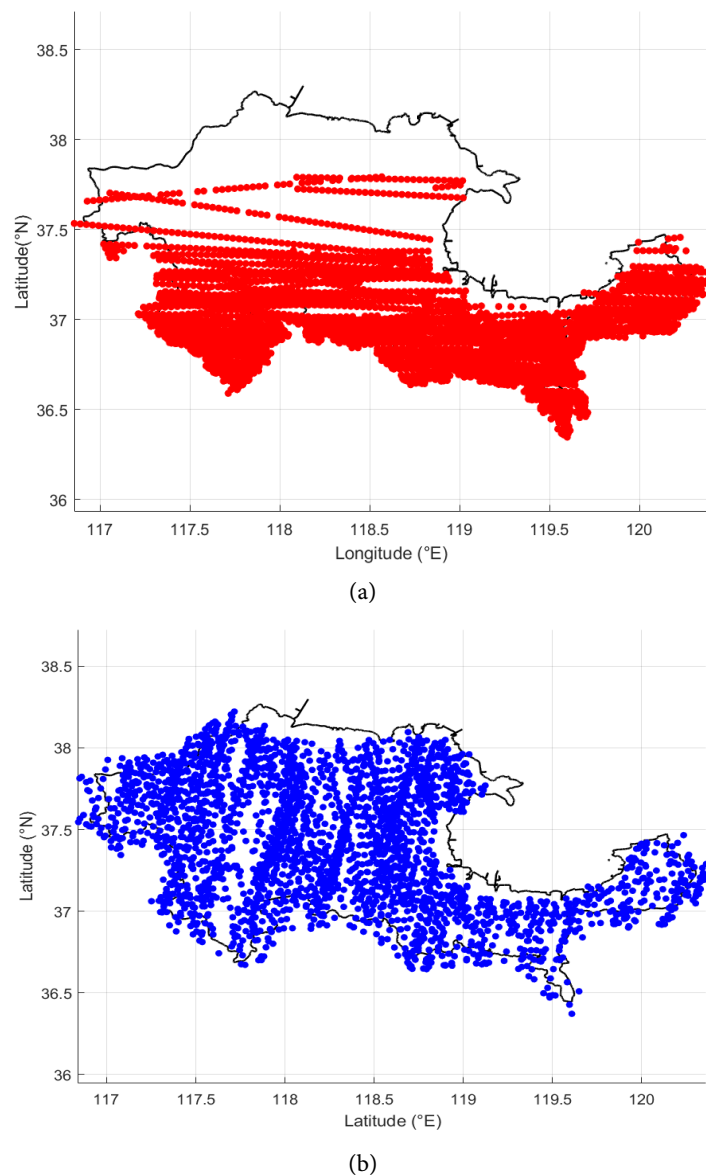
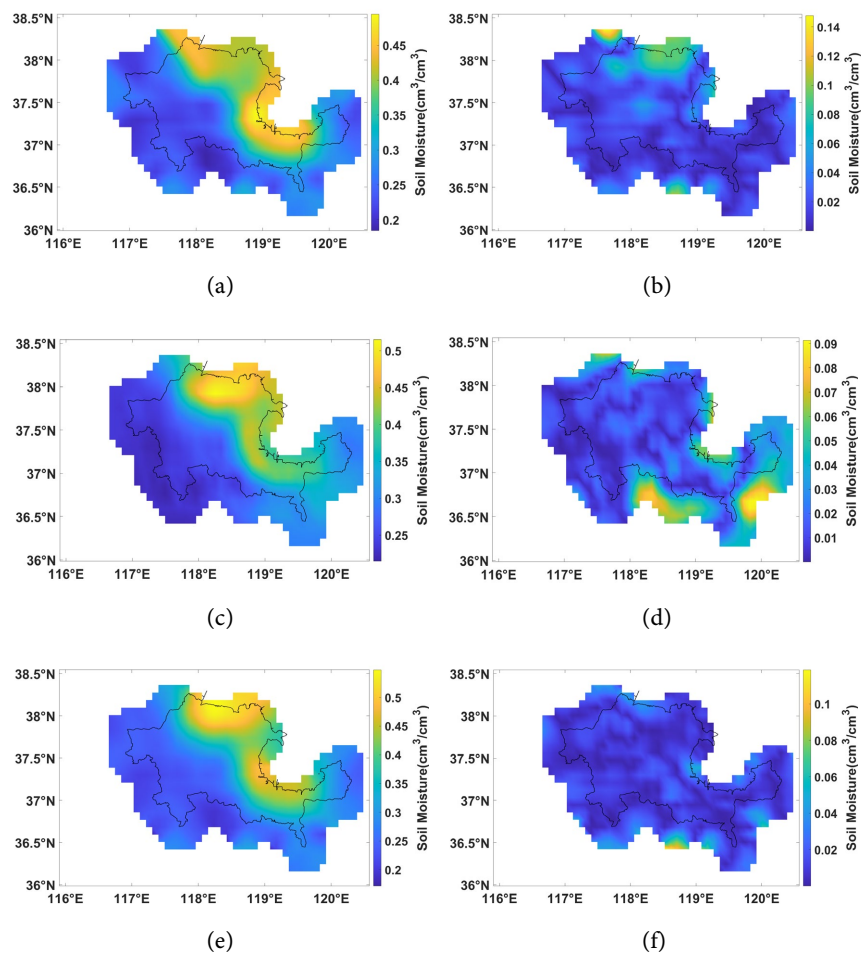


Figure 5. Distribution of satellite data (a) CYGNSS, (b) Tianmu.

This spatial distribution characteristic further confirms the necessity and scientific rationale for jointly using CYGNSS and Tianmu satellite data for soil moisture retrieval in this study.

However, since the model output is presented as a discrete point distribution, it cannot be directly compared pixel-by-pixel with the spatially continuous SMAP observation data. Therefore, this study introduces a spatial interpolation method to address this issue. Based on the longitude and latitude positions of the model prediction points, the interpolation algorithm transforms the discrete prediction results into continuous raster images that are consistent with the spatial resolution of SMAP data (9 km × 9 km). This approach ensures that the model predictions and SMAP observations can be accurately compared and evaluated on the same spatial scale.

Ultimately, **Figure 6** presents the predicted spatial distribution of soil moisture in the Yellow River Delta region for September 2023, after applying spatial interpolation. To quantitatively assess the model's retrieval performance, the correlation coefficient (R) and root mean square error (RMSE) between the predicted results and SMAP observations were calculated, and the detailed numerical results are summarized in **Table 2**.



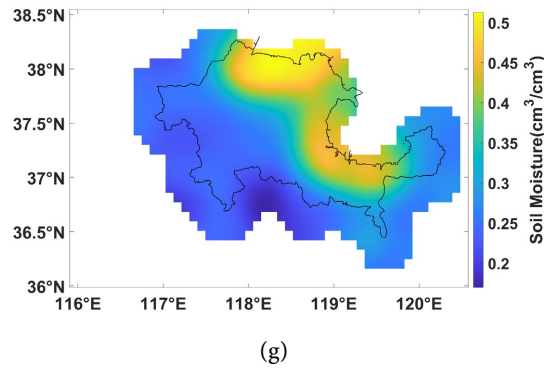


Figure 6. Soil moisture retrieval results of the model: (a) Prediction graph of CYGNSS, (b) Error graph of the predicted values of CYGNSS and SMAP, (c) Prediction graph of Tianmu, (d) Error graph of the predicted values of Tianmu and SMAP, (e) Combined prediction graph (f) The error plot of the combined predicted value and SMAP, (g) the truth plot of SMAP.

These quantitative indicators not only provide an objective evaluation of the overall prediction accuracy of the model but also highlight the improvement in soil moisture retrieval accuracy achieved by the combined use of CYGNSS and Tianmu satellite data.

Table 2. Accuracy indicators of the model prediction results.

Evaluation indicators	CYGNSS (8:2)	Tianmu (8:2)	CYGNSS (September)	Tianmu (September)	Joint (September)
R	0.9190	0.9083	0.8921	0.9219	0.9378
RMSE	0.0306	0.0419	0.0422	0.0363	0.0301

4.2. Discussion and Analysis

According to the accuracy indicators presented in **Table 2**, the TF-NET model shows a high overall accuracy in soil moisture retrieval within the Yellow River Delta region. In the experiment where the training and testing data were randomly split in an 8:2 ratio, the CYGNSS-based predictions achieved a correlation coefficient (R) of 0.9190 and a root mean square error (RMSE) of 0.0306 cm³/cm³. In contrast, the Tianmu-based predictions demonstrated slightly lower accuracy, with an R of 0.9083 and an RMSE of 0.0419 cm³/cm³. This discrepancy mainly arises because the Tianmu satellite has relatively fewer data points in the Yellow River Delta, leading to lower data coverage density, which limits the model's ability to capture complex spatial features.

To further assess the model's generalization capability, we conducted experiments using an independent dataset from September 2023 that was not involved in model training. In this case, the accuracy of both CYGNSS and Tianmu satellite predictions showed notable improvements. Specifically, the Tianmu satellite demonstrated a significant accuracy gain, with the correlation coefficient (R) increasing to 0.9219 and the RMSE decreasing to 0.0363 cm³/cm³. On the other

hand, the CYGNSS predictions for the same period resulted in an R of 0.8921 and an RMSE of $0.0422 \text{ cm}^3/\text{cm}^3$. This finding indicates that despite the limited data volume from the Tianmu satellite, its relatively uniform data distribution during the specific time window enables the model to capture feature patterns effectively, thus achieving better accuracy during independent month testing.

The most significant finding is that when the retrieval results from both CYGNSS and Tianmu satellites are combined, the model achieves substantially improved accuracy, with the correlation coefficient reaching 0.9378 and the RMSE dropping to $0.0301 \text{ cm}^3/\text{cm}^3$. This improvement is primarily due to the complementary spatial coverage of the two data sources. While CYGNSS data exhibits considerable gaps in the northern part of the Yellow River Delta, making it challenging to fully represent the spatial variability of soil moisture, the Tianmu satellite data effectively covers the areas where CYGNSS lacks information. This spatial complementarity between the two datasets enables the combined use of CYGNSS and Tianmu data to better represent the regional soil moisture distribution, significantly enhancing the model's prediction accuracy and robustness.

5. Conclusion

To address the challenge faced by existing soil moisture retrieval methods in effectively capturing the global features within the Delay-Doppler Map (DDM) when processing spaceborne GNSS-R data, this paper proposes a soil moisture retrieval method based on the Transformer Fusion Network (TF-NET). TF-NET utilizes the multi-head self-attention mechanism to perform deep feature extraction from CYGNSS and Tianmu satellite data separately, while the cross-attention mechanism enhances the feature correlation between auxiliary data and DDM data. Experimental results from the Yellow River Delta region demonstrate that this method can more effectively capture the global contextual information within GNSS-R data, achieving outstanding accuracy in soil moisture retrieval. Additionally, since CYGNSS and Tianmu satellite data exhibit complementary spatial coverage, combining their prediction results spatially further improves the overall performance of the model.

Funding

This work was supported by the Key Program of Joint Fund of the National Natural Science Foundation of China and Shandong Province under Grant U22A20586, the Natural Science Foundation of Shandong Province under Grant ZR2022MD015, the Fundamental Research Funds for the Central Universities under Grant 24CX02030A, the National Natural Science Foundation of China under Grant 41701513, 61371189, and 41772350, and the Key Research and Development Program of Shandong Province under Grant 2019GGX101033.

Acknowledgements

We extend our sincere gratitude to NASA for the provision of CYGNSS data and

SMAP data, as well as to the Tianmu Satellite team for providing the Tianmu satellite data.

Conflicts of Interest

The authors declare no conflicts of interest regarding the publication of this paper.

References

- [1] Bolten, J.D., Crow, W.T., Zhan, X., Jackson, T.J. and Reynolds, C.A. (2010) Evaluating the Utility of Remotely Sensed Soil Moisture Retrievals for Operational Agricultural Drought Monitoring. *IEEE Journal of Selected Topics in Applied Earth Observations and Remote Sensing*, **3**, 57-66. <https://doi.org/10.1109/jstars.2009.2037163>
- [2] Pablos, M., Martinezfernandez, J. and Sanchez, N. (2017) Temporal and Spatial Comparison of Agricultural Drought Indices from Moderate Resolution Satellite Soil Moisture Data over Northwest Spain. *Remote Sensing*, **9**, 1168-1179.
- [3] Piles, M., Petropoulos, G.P. and Sánchez, N. (2016) Towards Improved Spatiotemporal Resolution Soil Moisture Retrievals from the Synergy of SMOS and MSG SEVIRI Spaceborne Observations. *Remote Sensing of Environment*, **180**, 403-417.
- [4] UNDRR (2019) Global Assessment Report on Disaster Risk Reduction. United Nations Office for Disaster Risk Reduction.
- [5] Torres, R., Snoeij, P. and Geudtner, D. (2012) GMES Sentinel-1 Mission. *Remote Sensing of Environment*, **120**, 9-24.
- [6] Zavorotny, V.U., Gleason, S., Cardellach, E. and Camps, A. (2014) Tutorial on Remote Sensing Using GNSS Bistatic Radar of Opportunity. *IEEE Geoscience and Remote Sensing Magazine*, **2**, 8-45. <https://doi.org/10.1109/mgrs.2014.2374220>
- [7] Santi, E., Paloscia, S., Pettinato, S., Fontanelli, G., Clarizia, M.P., Guerriero, L., et al. (2019) Forest Biomass Estimate on Local and Global Scales through GNSS Reflectometry Techniques. 2019 *IEEE International Geoscience and Remote Sensing Symposium*, Yokohama, 28 July-2 August 2019, 8680-8683. <https://doi.org/10.1109/igarss.2019.8899140>
- [8] Rodriguez-Alvarez, N., Holt, B., Jaruwatanadilok, S., Podest, E. and Cavanaugh, K.C. (2019) An Arctic Sea Ice Multi-Step Classification Based on GNSS-R Data from the TDS-1 Mission. *Remote Sensing of Environment*, **230**, Article ID: 111202. <https://doi.org/10.1016/j.rse.2019.05.021>
- [9] Li, W., Cardellach, E., Fabra, F., Ribo, S. and Rius, A. (2020) Assessment of Spaceborne GNSS-R Ocean Altimetry Performance Using CYGNSS Mission Raw Data. *IEEE Transactions on Geoscience and Remote Sensing*, **58**, 238-250. <https://doi.org/10.1109/tgrs.2019.2936108>
- [10] Yan, Q., Huang, W., Jin, S. and Jia, Y. (2020) Pan-Tropical Soil Moisture Mapping Based on a Three-Layer Model from CYGNSS GNSS-R Data. *Remote Sensing of Environment*, **247**, Article ID: 111944. <https://doi.org/10.1016/j.rse.2020.111944>
- [11] Senyurek, V., Lei, F., Boyd, D., Kurum, M., Gurbuz, A.C. and Moorhead, R. (2020) Machine Learning-Based CYGNSS Soil Moisture Estimates over ISMN Sites in CONUS. *Remote Sensing*, **12**, Article No. 1168. <https://doi.org/10.3390/rs12071168>
- [12] Santi, E., Pettinato, S., Paloscia, S., Clarizia, M.P., Dente, L., Guerriero, L., et al. (2020) Soil Moisture and Forest Biomass Retrieval on a Global Scale by Using CyGNSS Data and Artificial Neural Networks. 2020 *IEEE International Geoscience and Remote Sensing Symposium*, Waikoloa, 26 September-2 October 2020, 5905-5908.

- <https://doi.org/10.1109/igarss39084.2020.9323896>
- [13] Al-Khaldi, M.M., Johnson, J.T., O'Brien, A.J., Balenzano, A. and Mattia, F. (2019) Time-Series Retrieval of Soil Moisture Using CYGNSS. *IEEE Transactions on Geoscience and Remote Sensing*, **57**, 4322-4331. <https://doi.org/10.1109/tgrs.2018.2890646>
- [14] Chew, C.C. and Small, E.E. (2018) Soil Moisture Sensing Using Spaceborne GNSS Reflections: Comparison of CYGNSS Reflectivity to SMAP Soil Moisture. *Geophysical Research Letters*, **45**, 4049-4057. <https://doi.org/10.1029/2018gl077905>
- [15] Kim, H. and Lakshmi, V. (2018) Use of Cyclone Global Navigation Satellite System (CyGNSS) Observations for Estimation of Soil Moisture. *Geophysical Research Letters*, **45**, 8272-8282. <https://doi.org/10.1029/2018gl078923>
- [16] Clarizia, M.P., Pierdicca, N., Costantini, F. and Floury, N. (2019) Analysis of CYGNSS Data for Soil Moisture Retrieval. *IEEE Journal of Selected Topics in Applied Earth Observations and Remote Sensing*, **12**, 2227-2235. <https://doi.org/10.1109/jstars.2019.2895510>
- [17] Dai, S., Song, D. and Wang, B. (2025) CT-NET: A Cross-Modal Transformer Network for Satellite-Borne GNSS-R Soil Moisture Retrieval. *International Conference on Remote Sensing and Digital Earth (RSDE 2024)*, Volume 13514, 135140S. <https://doi.org/10.1117/12.3059047>